

TEVATRON JET PHYSICS

F. CHLEBANA, FOR THE CDF AND DØ COLLABORATIONS

*Fermilab, MS 318, PO Box 500, Batavia, IL 60510-5011, USA**E-mail: chlebana@fnal.gov*

Preliminary jet measurements are presented from the CDF and DØ experiments at the Tevatron $p\bar{p}$ collider operating at a center of mass energy of 1.96 TeV. The increased center of mass energy together with about twice the integrated luminosity allows the inclusive jet cross section measurement to be extended by about 150 GeV. Preliminary measurements of the dijet azimuthal correlation for jets in the central rapidity region and the dijet mass distribution measured by the DØ collaboration are presented. Within the errors, the results are consistent with the predictions of NLO QCD.

1 Introduction

The Tevatron is currently the world's highest energy collider and is able to probe distance scales down to 10^{-17} cm. The study of jet production in high energy interactions tests our understanding of the Standard Model and allows us to search for new physics which could show up as an excess in the expected jet production rate. Particle structure is parameterized in terms of Parton Density Functions (PDFs) giving the probability of probing the constituent partons. The PDFs are universal and once known as a function of the kinematic variable x at a given Q^2 , can be evolved to different Q^2 values and used to predict the cross section for many processes at different energies. As experiments probe new regions of the kinematic phase space they provide ad-

ditional input for global QCD fits resulting in more precise PDFs with greater predictive power. The increase of the center of mass energy from 1.8 to 1.96 TeV results in an greater cross section at high E_T and this together with the higher operating luminosity of the Tevatron helps us to extend our reach to higher E_T values or equivalently shorter distance scales.

Both the CDF ¹ and DØ detectors ² have been upgraded in order to operate at the higher luminosity in Run II. The read-out electronics has been replaced in order to handle the smaller bunch spacing going from 3.56 μ s to 396 ns. CDF has installed a new central tracking chamber as well as a new silicon vertex detector. The online trigger has been upgraded giving CDF the capability of triggering on tracks at the first trigger stage and to select events with a displaced vertex at the second trigger stage. The DØ upgrades greatly improve the tracking capability providing momentum determination and vertexing for tracks with $|\eta| < 3$. DØ has installed a new silicon detector and fiber tracker surrounded by a 2 Tesla solenoid. The addition of a preshower detector surrounding the solenoid aids in electron identification and triggering and allows for the correction of electromagnetic energy for effects of the solenoid.

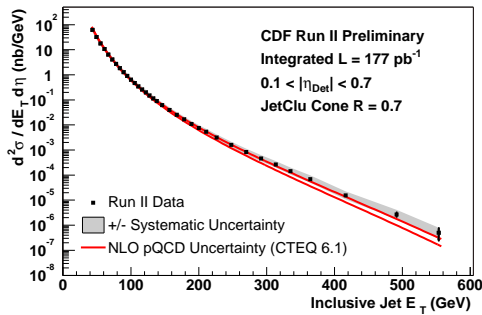


Figure 1. The inclusive jet cross section measured using the Run I clustering algorithm by CDF.

1.1 Jet Algorithms and the Inclusive Jet Cross Section

Preliminary results for the inclusive jet cross section from CDF using the Run I clustering algorithm³ are shown in Figure 1. The data are compared with the NLO calculation of JETRAD⁴ using the CTEQ5L⁵ PDF. The uncertainty resulting from the PDFs is shown as the two curves while the systematic error on the data is shown as the shaded band. Both experiments are now making use of improved jet clustering algorithms, such as Kt Clustering and MidPoint⁶, which will allow more direct comparisons between data and theory as well as between CDF and DØ. The cross section measurement from CDF using the Kt Clustering algorithm is shown in Figure 2 where the ratio of data over theory is plotted. The theory has not been corrected for the effects of hadronization or from the underlying event. These corrections are largest at low p_T and when applied to the theory will raise the predicted cross section so that the agreement between measurement and theory in the low p_T region becomes better. The size of the correction is dependent on the jet algorithm and needs to be properly modeled. DØ has measured the inclusive jet cross section in three rapidity, y , bins using the MidPoint clustering algorithm as shown

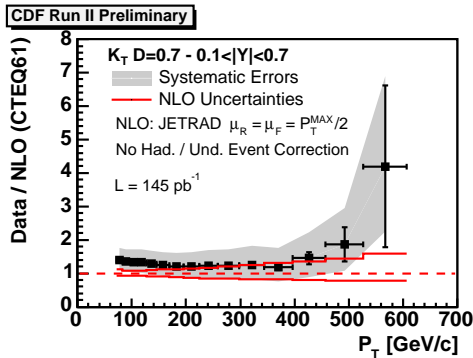


Figure 2. The ratio of data/theory for the inclusive jet cross section measured using the Kt Clustering algorithm.

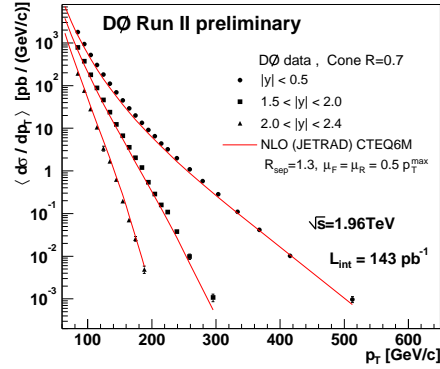


Figure 3. The inclusive jet cross section in different rapidity bins.

in Figure 3. Jet measurements in the forward y region provides input for global QCD PDF fits at lower x values. The dominant contribution to the systematic error results from the uncertainty on the energy scale. The inclusive jet cross section for the central rapidity region, $|y| < 0.5$, is compared to the theory prediction in Figure 4. As the p_T spectrum becomes steeper with increasing y , the energy scale error translates into a greater error on the cross section measurement. Within the large errors the results are in agreement with the QCD prediction. As the understanding of the detector improves we can expect that the systematic errors will be reduced.

Many classes of new particles have a larger branching fraction into just two partons than into modes including a lepton or electroweak gauge bosons. Such new particles could show up as a resonance in the dijet mass spectrum. Figure 5 shows the corrected dijet mass distribution measured by DØ. The preliminary results agree with the QCD prediction.

1.2 Dijet Azimuthal Correlations

Measurement of the correlations between the two leading jets in multijet production is sen-

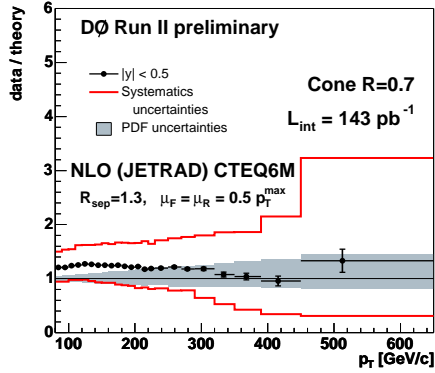


Figure 4. Ratio of data/theory for the inclusive jet cross section measured in the central rapidity region ($y < 0.5$).

sitive to the impact of QCD radiation. Additional jets produced at higher orders result in a decorrelated angle ($\Delta\phi_{dijet} < \pi$) between the two leading jets. There are several advantages of the $\Delta\phi_{dijet} < \pi$ measurement, it is simpler to define and understand, it is easier to measure a jet direction than its energy and the angular distribution $\Delta\phi$ is directly sensitive to higher order QCD radiation without explicitly having to measure a third jet. DØ has measured the angular distribution ⁷ in four different p_T regions and compared the results to pQCD in fixed order α_s (LO and NLO) calculated using NLO-JET++ ⁸ with the CTEQ6.1M PDFs. As expected the agreement with the LO calculation is poor while the NLO calculation provides a much better description of the data. Monte Carlo event generators, such as PYTHIA and HERWIG, use $2 \rightarrow 2$ LO pQCD matrix elements with phenomenological parton-shower models to simulate higher order QCD effects. The maximum p_T in the initial-state parton shower is directly related to the maximum virtuality and can be adjusted in PYTHIA. The effect on the angular distribution resulting from changing this parameter is shown as the shaded bands in Figure 6. Results are presented for the The low-

est ($75 < p_T < 100$) and highest ($p_T > 180$) p_T bins that were measured. The band covers the range when the maximum virtuality is increased from the default value by a factor of four and illustrates the potential for future efforts to tune the event generators.

Summary

The new detector and triggering capabilities of CDF and DØ build on the experience of Run I and greatly extend the physics capabilities. The performance of the Tevatron is rapidly improving and the maximum obtained average initial luminosity of $92 \times 10^{30} \text{ cm}^{-2} \text{ s}^{-1}$ has exceeded the Run IIa design goal. Several preliminary results have been presented based on a data sample of more than twice that of previously published results enabling us to extend the high E_T measurements by about 150 GeV. The additional material in front of the calorimeter resulting from the upgrades to the tracking systems requires that both experiments reevaluate the calorimeter response. The dominant source of systematic error results from the uncertainty of the energy scale and so far has been conservatively quoted. The results presented are consistent with the QCD predictions within the relatively large preliminary

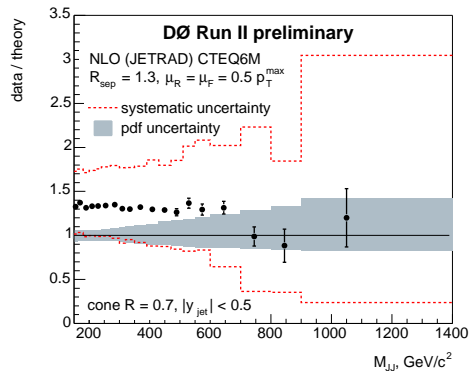


Figure 5. The ratio of the measured dijet cross section over the NLO pQCD calculation.

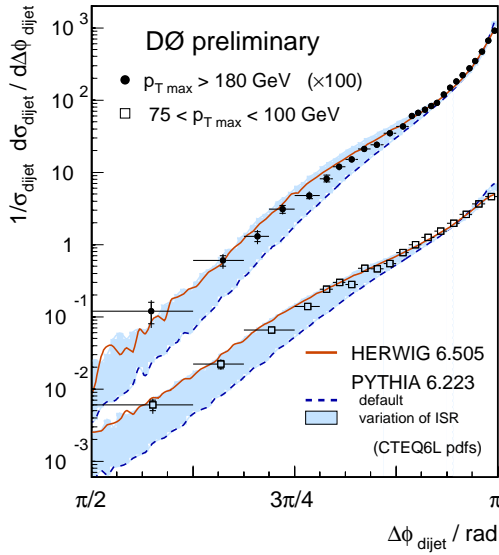


Figure 6. Angular correlation between the two leading jets is compared to the LO and NLO prediction using NLOJET++.

errors.

Acknowledgments

We thank the staffs at Fermilab and collaborating institutions, and acknowledge support from the Dept. of Energy, National Science Foundation, A.P. Sloan Foundation, Civilian Research and Development Foundation, Research Corporation, Texas Advanced Research Program, and the Alexander von Humboldt Foundation (USA); CONICET and UBACyT (Argentina); CAPES, CNPq, FAPERJ, FAPESP and FUNDUNESP (Brazil); Natural Sciences and Engineering Research Council and WestGrid Project (Canada); National Science Council (PRC); Colciencias (Colombia); Ministry of Education (Czech Republic); Human Potential Programme under contract HPRN-CT-20002, Probe for New Physics (EU); Commissariat à l'Energie Atomique and CNRS/Institut National de Physique Nucléaire et de Physique des Particules (France); BMMF and DFG (Ger-

many); Depts. of Atomic Energy and Science and Technology (India); Istituto Nazionale di Fisica Nucleare (Italy); Ministry of Education, Culture, Sports, Science and Technology (Japan); Science and Engineering Foundation, Research Foundation (Korea); CONACyT (Mexico); Foundation for Fundamental Research on Matter (The Netherlands); Ministry of Education and Science, Agency for Atomic Energy, Foundation for Basic Research and the RF President Grants Program (Russia); Comisión Interministerial de Ciencia y Tecnología (Spain); National Science Foundation (Switzerland); PPARC and the Royal Society (UK); and the Research Fund of Istanbul University Project No. 1755/21122001.

References

1. The CDF Collaboration, FERMILAB-PUB-96-390-E; A. Sill *et al.*, *Nucl. Instrum. Meth. A* **447**, 1 (2000); T. Affolder *et al.*, The CDF Collaboration, FERMILAB-PUB-03-355-E, submitted to *Nucl. Instrum. Meth. Phys. Res. A*; *Nucl. Instrum. Meth. A* **518**: 39-41, 2004;
2. V. Abazov *et al.*, (DØ Collaboration), in preparation for submission to *Nucl. Instrum. Methods Phys. Res. A*; T. LeCompte and H.T. Diehl, *Ann. Rev. Nucl. Part. Sci.* **50**, 71 (2000); S. Abachi *et al.*, (DØ Collaboration), *Nucl. Instrum. Methods Phys. Res. A* **338**, 185 (1994);
3. J. Huth *et al.*, "Proceedings 1990 Summer Study on High Energy Physics", ed. E. Berger, Singapore, World Scientific, 134 (1992); T. Affolder *et al.*, (CDF Collaboration), *Phys. Rev. D* **64**, 032001 (2001).
4. W. T. Giele, E. W. N. Glover and D. A. Kosower, *Nucl. Phys. B* **403**, 633 (1993).
5. H. L. Lai *et al.*, *Eur. Phys. J. C* **12**,

- 375 (2000)
6. G.C. Blazey et al., Proceedings of the Workshop: “QCD and Weak Boson Physics in Run II”, ed. U. Bauer, R.K. Ellis and D. Zeppenfeld, Batavia, IL., hep-ex/0005012.
 7. V.M. Abazov, et al (DØ Collaboration), hep-ex/0409040, Submitted to Phys. Rev. Lett.
 8. Z. Nagy, *Phys. Rev. Lett.* **88**, 122003 (2002); Z. Nagy, *Phys. Rev. D* **68**, 094002 (2003).